

An enzyme-free electrochemical immunosensor based on MOF/SWCN nanocomposites for rapid and sensitive detection of fibroblast growth factor 21

Tianxiao Yu¹, Shikuan Hou², Xizhenzi Fan¹, Yanxia Qiao³, Guohua Zhang⁴, Lingli Wang¹, Jun Ge^{1,*}

¹ Research center for clinical medical sciences, The Fourth Hospital of Shijiazhuang (The Affiliated Obstetrics and Gynecology Hospital of Hebei Medical University), Shijiazhuang, 050000, China.

² Department of clinical laboratory, The Fourth Hospital of Shijiazhuang (The Affiliated Obstetrics and Gynecology Hospital of Hebei Medical University), Shijiazhuang, 050000, China.

³ Department of neonatology, The Fourth Hospital of Shijiazhuang (The Affiliated Obstetrics and Gynecology Hospital of Hebei Medical University), Shijiazhuang, 050000, China.

⁴ Department of obstetrics and gynecology, The Fourth Hospital of Shijiazhuang (The Affiliated Obstetrics and Gynecology Hospital of Hebei Medical University), Shijiazhuang, 050000, China.

*E-mail: 404828162@qq.com

Received: 15 May 2022 / Accepted: 6 July 2022 / Published: 7 August 2022

In this work, an enzyme-free electrochemical immunosensor based on metal-organic framework (MOF) and single-wall carbon nanotube (SWCN) nanocomposite coated glassy carbon electrode (GCE) for rapid and sensitive detection of fibroblast growth factor 21 (FGF-21) was proposed. The synthesized MOF/SWCN were characterized by transmission electron microscopy (TEM). It exhibited high-speed charge mobility, excellent conductivity and high surface area, significantly amplifying the current signal response. Furthermore, to immobilize the FGF-21 capture antibody on the MOF/SWCN electrode surface in an ordered orientation, staphylococcal protein A (SPA) was introduced as a connecting element, which significantly increased the antigen-binding ability and immunosensor stability. Under optimal conditions, the wide linear range of the immunosensor was 1.00 pg mL⁻¹ to 500 ng mL⁻¹, with a low detection limit was 0.35 pg mL⁻¹. Additionally, the immunosensor also showed excellent reproducibility and selectivity. It was also successfully used to detect FGF-21 in human serum samples with satisfying recoveries. Thus, the strategy provides a simple and sensitive method for FGF-21 detection, indicating significant potential applications in clinical diagnostics.

Keywords: Electrochemical immunosensor; MOF/SWCN; Staphylococcal protein A; Fibroblast growth factor 21

1. INTRODUCTION

The diagnosis of mitochondrial diseases remains challenging due to clinical and genetic heterogeneity [1, 2]. Several studies have shown that fibroblast growth factor 21 (FGF-21) can be used

as a reliable serum biomarker to diagnose mitochondrial diseases. It can improve and simplify the diagnostic procedures and reduce the need for muscle biopsy [3, 4]. The typical detection method for FGF-21 is enzyme-linked immunosorbent assay (ELISA). However, the detection limit of most ELISA kits is between 15 pg mL^{-1} to 20 pg mL^{-1} (Solarbio life sciences Co., Ltd (Beijing), Fein sciences Co., Ltd (Wuhan), Sangon Biotech Co., Ltd (Shanghai)) and the detection time is usually more than 2 hours, which is far from meeting the needs of clinical detection.

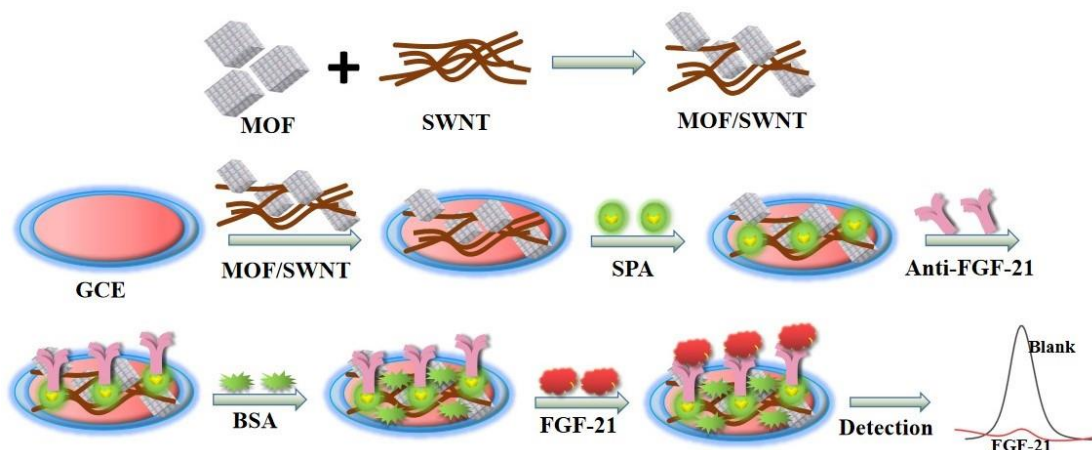
Electrochemical immunosensors were mainly used for biomarkers detection because of their simple operation, economic cost, and fast analysis [5, 6]. The design and selection of signal amplification strategies are significant for developing highly sensitive electrochemical immunosensor [7]. In recent years, electrochemical immunosensor based on functionalized nanomaterials has been proved to be a promising signal amplification method, which provides a lower detection limit for analytes [8-10]. Therefore, it is an imperative choice to develop novel functionalized nanomaterials to design more excellent signal amplification strategies.

Metal-organic framework (MOF) is a kind of coordination polymer which is continuously connected by organic linkers and inorganic metal ions in a highly oriented structure [11]. MOF as a labelled nanomaterial has been used in the field of biosensing. Among various MOFs, Fe based MOF may be highly suitable for biological analysis because of their environmental friendliness and low cost [12, 13]. The Fe-MOF also has unique properties, such as an ultra-high specific surface area with large tunable pores, dense catalytic sites and appropriate surface functional groups [14]. Furthermore, it can also enhance the stability and activity of binding biomolecules [15]. However, MOFs are inherently poor conductors and have low stability in water mediums [16]. Therefore, few studies have been reported about electrochemical immunosensors with MOF matrix modified electrodes and immobilized protein molecules. Here, to enhance Fe-MOF's electrical conductivity and antibody sites, we fabricated nanocomposites of Fe-MOF and single-wall carbon nanotubes (SWCN). The synthesized MOF/SWCN was used to manufacture an enzyme-free electrochemical immunosensor for FGF-21 detection, improving detection sensitivity.

Furthermore, the immobilized antibodies with well-defined orientation can significantly increase the antigen-binding ability and improve the function of the detection system [17, 18]. Staphylococcal protein A (SPA) is of great significance as a powerful immunological tool because it can closely bind to the Fc region of IgG antibodies [19, 20]. The anti-FGF-21 antibody is a recombinant version of human IgG that recognizes the FGF-21 protein. In this work, the antibody would be positioned on the SPA surface in an appropriate orientation to bind to the antigen, further improving the stability and sensitivity of the immunosensor.

Based on the above discussions, this study describes a simple and cost-effective enzyme-free electrochemical immunosensor for detecting FGF-21 to significantly improve the sensitivity, specificity, stability and detection efficiency during the diagnosis of mitochondrial diseases. In the work, the MOF/SWCN enhanced the electrical conductivity of the glassy carbon electrode (GCE) and produced appropriate high density immobilizing sites. SPA modified on the GCE/MOF/SWCN surface ensured the orientation of the specific FGF-21 IgG antibodies. The comprehensive advantages of each component of MOF/SWNT lead to the formation of biocompatible surfaces with enhanced electrochemical properties. The sensitivity, stability and accuracy of the immunosensor had been greatly

improved. Furthermore, this immunosensor doesn't require sample pre-treatment or labelling, nor does it require a large volume of samples. In addition, the developed immunosensor was used to detect FGF-21 in serum samples and obtained satisfactory results. The biosensor has great application potential in clinical protein detection and will stimulate the future development of enzyme-free electrochemical biosensors for protein detection in clinical diagnostics.



Scheme 1. Schematic for the electrochemical detection of FGF-21 protein based on MOF/SWCN nanocomposites.

2. EXPERIMENTAL

2.1 Reagents and materials

Recombinant human FGF-21 protein and anti-FGF-21 antibody were purchased from Proteintech (Wuhan, China). Fe-MOF and Carboxylated SWCN were purchased from Xianfeng nanomaterials technology Co., Ltd. (Nanjing, China). N, N-dimethylformamide (DMF) and formic acid were acquired from Aladdin-reagent (Shanghai, China); SPA and bovine serum albumin (BSA) were obtained from Solarbio life sciences (Beijing, China).

2.2 Instruments

All electrochemical measurements were performed on an electrochemical workstation (CHI 760E, Chenhua, China). A classical three-electrode system was used with a GCE as the working electrode, an Ag/AgCl electrode as the reference electrode, and a platinum wire as the counter electrode. MOF/SWCN nanocomposites' surface morphologies were characterized by transmission electron microscopy (TEM, JEM-2100, Japan).

2.3 Synthesis of MOF/SWCN

100 mg SWCN was added to a 40 mL 1:1 (v/v) mixture of DMF and formic acid, then ultrasonic

treatment for 30 minutes to obtain a uniform dispersion. After that, 100 mg of Fe-MOF was added to the above solution and sonicated for another 30 minutes. The grey mass was collected by centrifugation for 15 minutes (12000 rpm), washed three times with DMF and methanol, and then dried in a vacuum at 70 °C for 2 hours.

2.4 Preparation of the electrochemical immunosensor

The GCE was polished with aluminium oxide powder and then washed three times with ethanol and ultrapure water to obtain a clean mirror surface. The MOF/SWCN mixed solution (1.0 mg mL⁻¹) was uniformly drop-coated on the GCE surface. After drying, 10 µL of SPA (5.0 mg mL⁻¹) in PBS buffer was dropped onto the GCE/MOF/SWCN surface for 45 minutes to immobilize the SPA molecules. After washing with PBS buffer, 10 µL of anti-FGF-21 antibody (10 µg mL⁻¹) in PBS buffer was cast onto the GCE/MOF/SWCN/SPA surface for 40 minutes to bind onto the electrode surface in an orderly direction through SPA. Subsequently, 10 µL of BSA (1%) solution was dropped onto the modified electrode to block the available active sites and nonspecific interaction. After each step, the electrode was thoroughly rinsed with PBS to remove unbound molecules. Then, the electrochemical immunosensor was stored at 4 °C for future use.

2.5 Electrochemical measurements

A differential pulse voltammogram (DPV) was used in performance testing. Besides, to investigate the repeatability of the sensor, each sample was tested three times. 10 µL of each solution containing different concentrations of FGF-21 protein was separately dropped on the immunosensor. After incubation at 37 °C for 30 minutes, PBS buffer was used to rinse the unbound molecules. Then, the DPV experiment analyzed the current signal response between -0.2V and 0.7 V in 5.0 mM [Fe(CN)₆]^{3-/4-} containing 0.1 M KCl in the bottom solution.

3. RESULTS AND DISCUSSION

3.1 Morphology characterization of MOF and MOF/SWCN

The morphology of the Fe-MOF, SWCN and MOF/SWCN nanocomposites were examined by transmission electron microscopy (TEM, JEM-2100, Japan). The TEM of Fe-MOF depicted nanometer-sized (300-600 nm) crystals shaped particles (Fig. 1a). The SWCN are tube bundles with uniform diameter distribution (Fig. 1b). The MOF/SWCN showed a crystal Fe-MOF anchored on the SWCN (Fig. 1c). All these above confirmed that we successfully synthesized the Fe-MOF and SWCN composites.

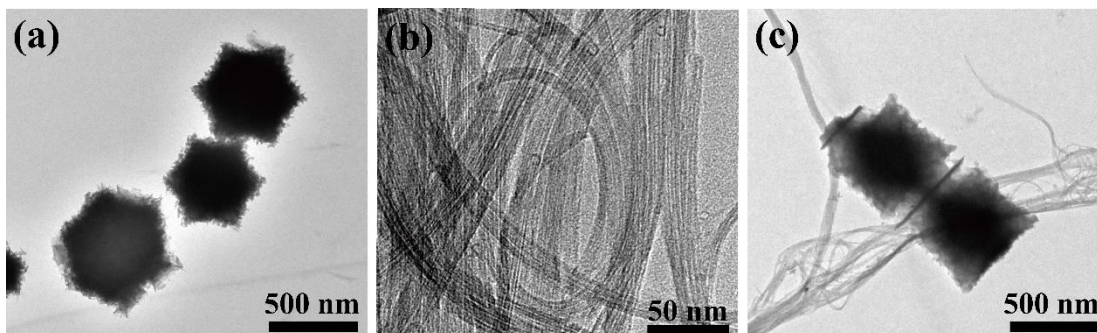


Figure 1. TEM image (a) Fe-MOF, (b) SWCN, (C) MOF/SWCN nanocomposites.

3.2 Electrochemical characterization

Each step of the immunosensor fabrication was characterized by EIS and CV in the substrate solution of 5.0 mM $[\text{Fe}(\text{CN})_6]^{3-/4-}$ containing 0.1 M KCl. First, the assembly of the immunosensor was verified by EIS. Fig. 2A showed that after depositing MOF/SWCN on the electrode, the Nyquist plot of GCE/MOF/SWCN (curve b) is significantly much lower than that of bare GCE (curve a). This is mainly because MOF/SWCN has excellent electrical conductivity and can accelerate electron transfer. It further confirms what was reported in previous article that MOF nanocomposites on electrode surface can enhance the sensor signals [21]. After that, SPA solution, anti-FGF-21 antibody, BSA, and FGF-21 protein were added dropwise to the electrode, and the response signals (curves c, d, e, f) of the electrode gradually increased, mainly because SPA, anti-FGF-21 antibody, BSA, and FGF-21 protein had been successfully bound to the electrode. These biological macromolecular proteins slowed down the transfer speed of electrons. The signal response verified by CV was consistent with the EIS results. The EIS and CV results fully proved the successful assembly of the sensor and further confirmed the feasibility of this strategy.

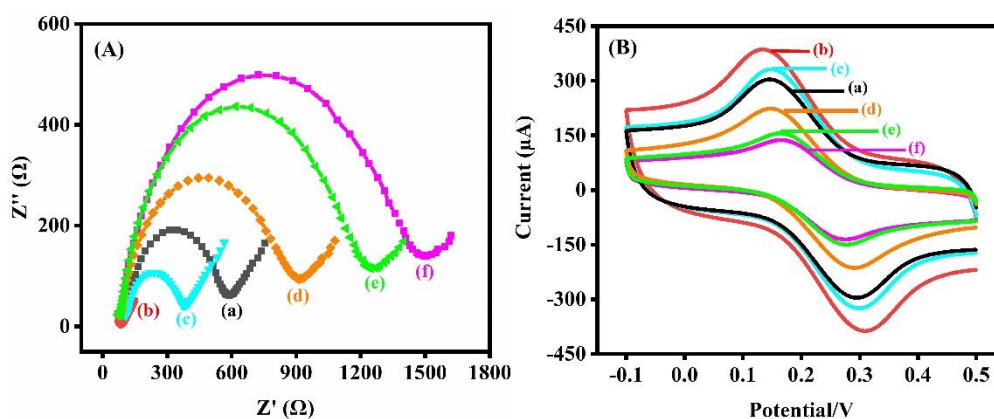


Figure 2. (A) Electrochemical impedance spectroscopy, (B) Cyclic voltammetry of different modification step on electrode surface in 5 mM $[\text{Fe}(\text{CN})_6]^{3-/4-}$ containing 0.1 M KCl solution. (a) Bare GCE, (b) GCE/MOF/SWCN, (c) GCE/MOF/SWCN/SPA, (d) GCE/MOF/SWCN/SPA/anti-FGF-21, (e) GCE/MOF/SWCN/SPA/anti-FGF-21/BSA, (f) GCE/MOF/SWCN/SPA/anti-FGF-21/BSA/FGF-21.

3.3 Optimization condition for detection of FGF-21

The CV current signal of the immunosensor in PBS solution containing 5 mM $[\text{Fe}(\text{CN})_6]^{3-/4-}$ and 0.1 M KCl (Fig. 3) were used to optimize several parameters in the fabrication process of the immunosensor. The amount of anti-FGF-21 antibody was an important parameter, as it can determine the sensitivity and linear range of detection. It can be seen from figure 3A that the optimal concentration of anti-FGF-21 antibody was $10 \mu\text{g mL}^{-1}$. Figure 3B showed that with the increased incubation time of SPA and anti-FGF-21, the peak current decreased gradually, up to 40 minutes and became steady afterwards. So, 40 minutes was chosen as the optimal time. Furthermore, the optimum binding time between anti-FGF-21 with FGF-21 was found as 30 minutes (Fig. 3C). All subsequent experiments were carried out according to these optimized conditions

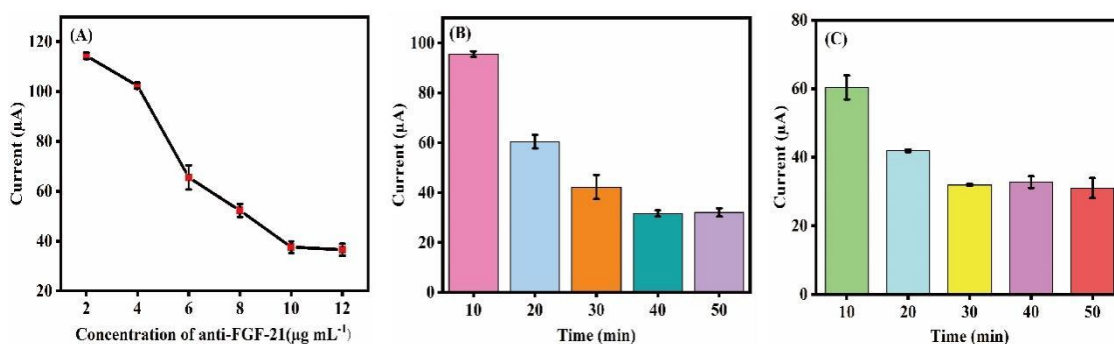


Figure 3. Optimization of assay conditions for the electrochemical detection of FGF-21. (A) Concentrations of anti-FGF-21 antibody, (B) Reaction time of SPA and anti-FGF-21 antibody, (C) Reaction time of anti-FGF-21 antibody and FGF-21 protein; (Concentration of FGF-21 were 500 ng mL^{-1} in Fig 3A, 3B, and 3C). Error bars show standard deviations of the three repeated experiments.

3.4 Analytical performance of the established sensing platform

Under the best experimental conditions, the electrochemical immunosensor was used to detect FGF-21 protein with different concentrations by DPV methods. With the increase in FGF-21 protein concentrations, the current response values gradually decreased (Fig. 4A, curve a-h). They showed a good linear relationship with the logarithmic concentration of FGF-21 from 1 pg mL^{-1} to 500 ng mL^{-1} (Fig. 4B). The linear relationship equation was described as $I (\mu\text{A}) = -12.49 \lg C (\text{ ng mL}^{-1}) + 36.30$ ($R^2 = 0.9984$), and the LOD was 0.35 pg mL^{-1} . The LOD of the designed immunosensor was greatly lower than that of the ELISA platform indicating the good sensitivity of our sensor [22]. Compared with the electrochemical immunosensor reported in the previous literature (Table 1), the proposed electrochemical immunosensor had a lower detection line, and wider detection range, which indicated that the biosensor established in this study has a great improvement in analytical performance due to the amplification strategy of MOF/SWCN modified GCE and SPA binding method.

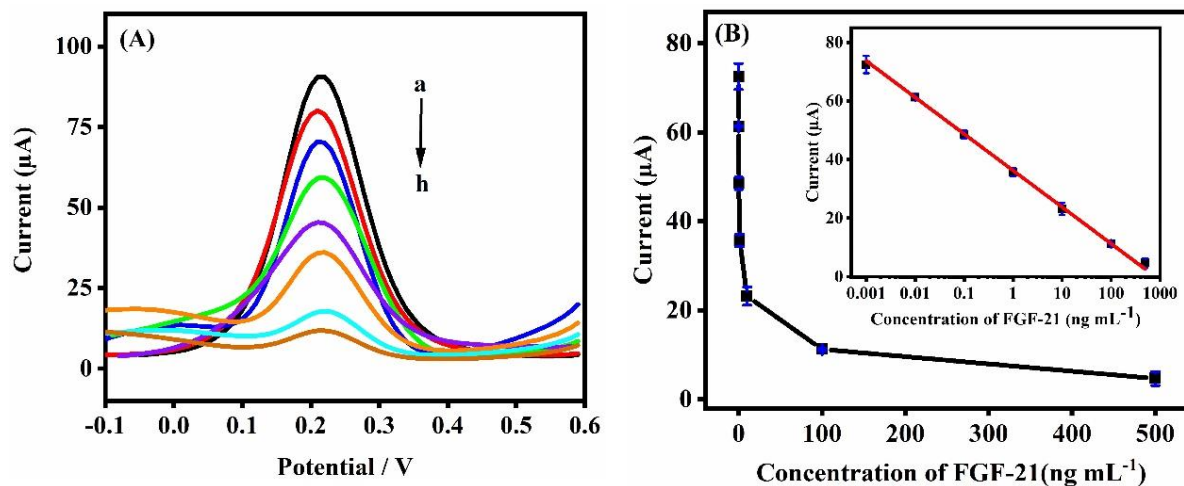


Figure 4 (A) DPV detection of FGF-21 with concentrations from 1 pg mL⁻¹ to 500 ng mL⁻¹. (a: Blank, b: 1 pg mL⁻¹, c: 10 pg mL⁻¹, d: 100 pg mL⁻¹, e: 1 ng mL⁻¹, f: 10 ng mL⁻¹, g: 100 ng mL⁻¹, h: 500 ng mL⁻¹); (B) DPV detection to different concentrations of FGF-21 protein (insert: Calibration curve of DPV currents vs logarithmic concentration of FGF-21).

Table 1. An overview on recently reported several electrochemical biosensors for determination of proteins.

Material	Method	Linear range (g/mL)	Detection limit (g/mL)	Ref.
Graphene@PdPtNPs	DPV	8.0×10^{-12} - 8.0×10^{-8}	2.5×10^{-12}	[23]
rGO/GC	EIS	1.0×10^{-10} - 5.0×10^{-9}	5.0×10^{-11}	[24]
PPD/GR	CV	1.0×10^{-9} - 1.0×10^{-6}	3.0×10^{-10}	[25]
Au-MoS ₂ /MOF	Amperometry	1.0×10^{-12} - 1.0×10^{-7}	3.7×10^{-13}	[26]
AgNPs/GQD	CV	1.0×10^{-11} - 4.0×10^{-7}	1.0×10^{-11}	[27]
MOF/SWCN/SPA	DPV	1.0×10^{-12} - 5.0×10^{-7}	3.5×10^{-13}	This work

3.5 Selectivity, stability, and reproducibility of the method

To avoid false recognition, it is essential to investigate the selectivity of immunosensor. Under the same experimental conditions, we compared the DPV response of the immunosensor towards the target FGF-21 protein and other interfering proteins such as AFP, CEA and BSA. As shown in Fig. 5, in the presence of target FGF-21, the DPV response significantly decreased. At the same time, no significant reduction was detected when detected other proteins, indicating that the immunosensor had reasonable specificity for target FGF-21 detection.

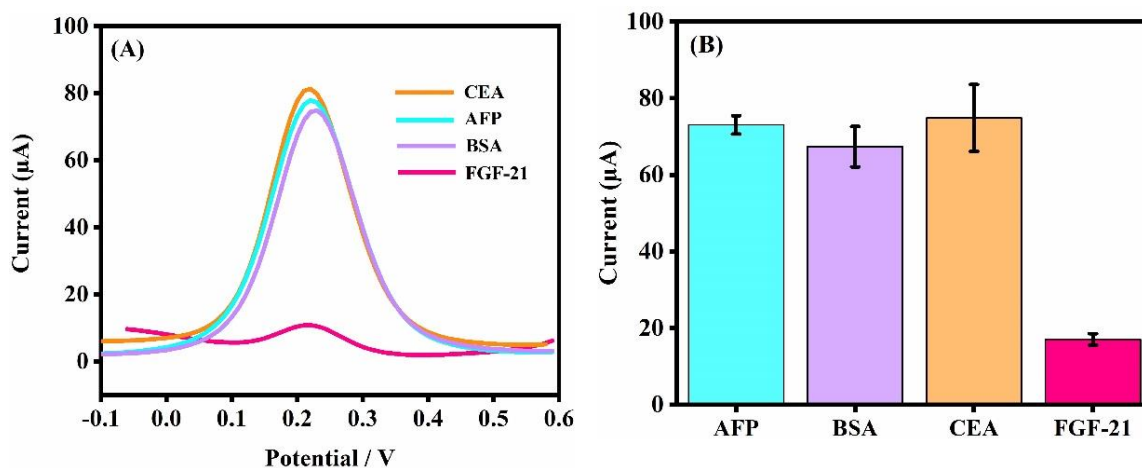


Figure 5. (A) DPV responses and (B) bar chart analysis of the immunosensor to 10 ng mL^{-1} of AFP, BSA, CEA and the target FGF-21.

The long-term stability of the immunosensor was also investigated. The electrode (GCE/MOF/SWCN/SPA/anti-FGF-21/BSA) was stored in a $4 \text{ }^{\circ}\text{C}$ refrigerator, and the target FGF-21 was measured after 7 days and 14 days, respectively. The results showed that the peak current retained 91.6% and 87.9% of its initial response, indicating that the immunosensor had good storage stability. The repeatability of the proposed immunosensor was studied by repeatedly measuring four spiked samples with different FGF-21 concentrations (100 pg mL^{-1} , 1 ng mL^{-1} , 10 ng mL^{-1} , 100 ng mL^{-1}) three times. The results showed that the relative standard deviation (RSD) of the electrochemical immunosensor was 1.38%-2.85%, which denoted excellent repeatability and accuracy. All these can be attributed to the antibody immobilization method on the electrode surface. The immobilized antibodies with well-defined orientation can greatly increase antigen-binding capacity and improve stability, and repeatability of the detection system [28].

3.6 Real sample analysis

To verify the feasibility of the designed immunosensor for detecting FGF-21, the immunosensor was investigated by measuring FGF-21 in serum of patients from The fourth hospital of Shijiazhuang. 1.0 mL of serum sample (confirmed to be free of FGF-21) was diluted 10 times with PBS buffer (pH 7.4). The target FGF-21 was spiked into the diluted serum with different concentrations, then determined by the proposed method. Table 2 showed that the spiked samples evaluated in each engagement illustrated high recovery percentages ranging from 95.8% to 114.0%, within the acceptable limits for ligand binding assays (80-120% recoveries) [29]. The method with a good RSD of 3.61% to 7.86%, indicating the immunosensor can be used for the detection of complicated biological samples with good precision.

Table 2. Detection of the FGF-21 in spiked samples by the proposed biosensor (n = 3)

Spiking value (g/mL)	Assayed value (g/mL)	Recovery (%)	RSD
1.00×10^{-9}	1.08×10^{-9}	100.82	7.86
1.00×10^{-8}	9.58×10^{-9}	95.84	4.01
1.00×10^{-7}	1.14×10^{-7}	114.01	3.61

4. CONCLUSIONS

Herein, we have offered an electrochemical immunosensor which was applied for rapid screening of FGF-21 with the aim of mitochondrial disease diagnosis. The GCE was modified with MOF/SWCN nanocomposites in biosensor fabrication to enhance the electrical conductivity and antibody sites. Then the SPA layer was used as a receptor element to immobilize the anti-FGF-21 IgG antibody in the regular direction. This biosensor had high sensitivity and wide linear range and could detect FGF-21 in 30 minutes without cross-reactivity when tested with other proteins. The results rely on some key features: the MOF/SWCN nanocomposites provide a suitable substrate and more active sites for SPA stabilization on the electrode surface; By loading a large amount of SPA and then loading anti-FGF-21 in an orderly direction, great amplified sensitivity and selectivity were obtained, the use of BSA blocks the available active sites, prevents nonspecific adsorption, and provides a specific sensing interface to avoid interference with other interfering species. The obtained results demonstrate that the immunosensor can be used as a promising clinical tool model for detecting FGF-21 with satisfactory results.

AUTHORSHIP CONTRIBUTION STATEMENT

Tianxiao Yu: Conceptualization, Methodology, Writing-original draft, Funding acquisition. Xizhenzi Fan: Conceptualization, Data curation. Yanxia Qiao: Conceptualization, Methodology. Guohua Zhang: Data curation, Formal analysis. Lingli Wang: Data curation, Formal analysis. Jun Ge: Resources, Project administration, Writing-review & editing.

FUNDING:

This work was financially supported by the Natural Science Foundation of Hebei Province in China (No. H2020106237).

CONFLICTS OF INTEREST

There are no conflicts to declare.

References

1. S. L. Stenton and H. Prokisch, *Essays Biochem*, 62 (2018) 399.
2. C. S. Chi, *Pediatr Neonatol*, 56 (2015) 7.
3. A. Huddar, P. Govindaraj and S. Chiplunkar, *Mitochondrion*, 60 (2021) 170.
4. R. L. Davis and C. Liang, *Neurology*, 81 (2013) 1819.
5. F. Mollarasouli, S. Kurbanoglu and S. A. Ozkan, *Biosensors-basel*, 9 (2019) 86.

6. W. Wen, X. Yan and C. Zhu, *Anal Chem*, 89 (2017) 138.
7. I. H. Cho, J. Lee and J. Kim, *Biosensors-basel*, 18 (2018) 207.
8. N. Wang, J. Wang and X. Zhao, *Talanta*, 226 (2021) 122133.
9. Y. Yang, Q. Yan and Q. Liu, *Biosens Bioelectron*, 99 (2018) 450.
10. A. Popov, B. Brasiunas and A. Kausaite-Minkstimiene, *Chemosensors*, 9 (2021) 85.
11. A. Pandey, N. Dhas and P. Deshmukh, *Coordin Chem Rev*, 409 (2020) 213212.
12. L. He, Y. Dong and Y. Zheng, *J Hazard Mater*, 361 (2019) 85.
13. H. Hu, H. X. Zhang, Y. Chen, Y. J. Chen and L. Zhuang, *Chem Eng J*, 368 (2019) 273.
14. J. Song, M. Huang and X. Lin, *Chem Eng J*, 427 (2022) 130913.
15. H. Dong, S. Liu and Q. Liu, *Biosens Bioelectron*, 195 (2022) 113648.
16. S. Biswas, Q. Lan and Y. Xie, *Mater. Interfaces*, 13 (2021) 3295.
17. Z. Rahmati, M. Roushani and H. Hosseini, *Microchimica Acta*, 188 (2021) 1.
18. E. Matysiak-Brynda, B. Wagner and M. Bystrzejewski, *Biosens Bioelectron*, 109 (2018) 83.
19. X. H. Yang, L. M. Huan and X. S. Chu, *Biochem Eng J*, 139 (2018) 15.
20. A. O. Bakhmachuk, O. B. Gorbatiuk and A. E. Rachkov, *Biopolymers and Cell*, 36 (2020) 271.
21. X. Zhang, R. Wang, Y. Wei, X. Pei, Z. Zhou, J. Zhang, R. Zhang and D. Zhang, *Int J Electrochem Sci*, 16 (2021) 210465.
22. H. H. Sunwoo, A. Palaniyappan, A. Ganguly, P.K. Bhatnagar, D. Das, A. O. El-Kadi, M. R. Suresh, *J Virol Methods*, 187 (2013) 72.
23. G. Zhang, Z. Liu, L. Fan, Y. Han, and Y. Guo, *Biosens Bioelectron*, 173 (2021) 112785.
24. M. Jozghorbani, M. Fathi, S. H. Kazemi, and N. Alinejadian, *Anal Chem*, 613 (2021) 114017.
25. A. Jafar, M. Mehdi, K. Alireza, S. N. Ali and R. N. Mehdi, *Anal Biochem*, 548 (2018) 53.
26. H. Dong, S. Liu, Q. Liu, Y. Li, Y. Li and Z. Zhao, *Biosens Bioelectron*, 195 (2022) 113648.
27. M. Jafari, M. Hasanzadeh, E. Solhi, S. Hassanpour, N. Shadjou, A. Mokhtarzadeh, A. Jouyban and S. Mahboob, *Int J Biol Macromol*, 126 (2019) 1255.
28. J. Zhou, L. Du and L. Sensors Actuators B Chem, 197 (2014) 220.
29. C. T. Viswanathan, S. Bansal, B. Booth, A. J. DeStefano, M. J. Rose, J. Sailstad, V. P. Shah, J. P. Skelly, P. G. Swann, R. Weiner, *Pharm Res*, 24 (2007) 1962.